

Two Methods for the Determination of Inertial Sensor Parameters

Vladimir Vukmirica¹⁾

Ivana Trajkovski¹⁾

Nada Asanović¹⁾

Inertial sensors, gyroscopes and accelerometers are widely applied. Inertial navigation systems (INS) usually consist of the inertial measuring unit (IMU) with three mutually perpendicular gyroscopes and accelerometers that represent three input axes to the system and navigation algorithm. Input values for the navigation algorithm are signals of gyroscopes and accelerometers. It is very important to know sources of navigation algorithm errors. One of the sources is a bias instability. A bias instability is a parameter that defines a class of sensors. The class of gyroscopes is defined in deg/h or deg/s and the class of accelerometers is defined in mg or μg . Other parameters defining a random walk of sensors are the angle random walk of gyroscopes and the velocity random walk of accelerometers. Although manufacturers declare these parameters in their data sheets, it is very important to confirm all declared sensor parameters before application. Two methods of angle random walk, velocity random walk and bias instability are presented and discussed with reference to their precision. These two methods are based on the Allan variance and power spectral density (PSD). The analysis was performed on the Analog Devices ADIS 16365 six degree of freedom sensor

Key words: navigation system, inertial system, inertial navigation, inertial sensor, gyroscope, accelerometer.

Introduction

TWO main parameters representing the quality of inertial sensors are the angle random walk and the bias instability for gyroscopes and the velocity random walk and bias instabilities for accelerometers. These two parameters should be obtained by the Allan variance method or by power spectral density.

To compare the two methods of determining inertial sensor parameters, the parameters of the Analog Devices ADIS 16365 [1] six degree sensor are determined. The angular random walk and the bias instability of gyroscopes as well as the velocity random walk and bias instability of accelerometers are determined [2]. The Allan variance method presented in [3], [4], [5], [6], [7] is used for developing an own software for signal analysis. The power spectral density signal analysis was made in MATLAB according to [3], [4], [8], [9] and [10].

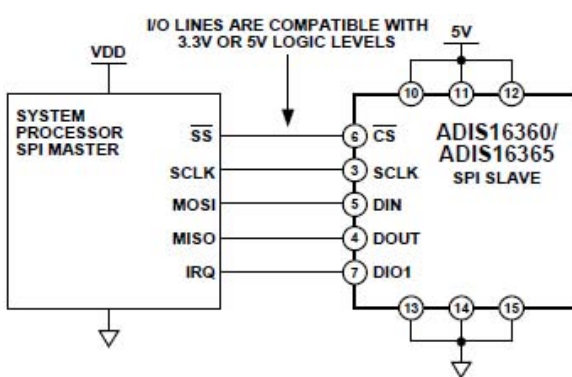


Figure1. Electrical connection diagram

According to a manufacturer scheme of a typical system application, the master processor PHILIPS ARM CORE 7 is used to access the output data registers through the SPI interface (Fig.1). The maximum sampling rate of data is 0.01s.

The sensor ADIS16365 operates as an SPI slave device that communicates with master processors. The SPI operates in a full duplex mode, which means that the master processor can read the output data from DOUT while using the same SCLK pulses to transmit the next target address on DIN [1].

The master processor reads the gyroscope output signal $\tilde{\omega}$ in deg/s and the accelerometer \tilde{a} output signals in g units.

Random walk and bias instability are the parameters presented in data sheet [1]. The sensors parameters are determined based on signals measured in accordance with a scheme (Fig.1).

Allan variance and power spectral density (PSD) are used for the identification of noise parameters

The sensors parameters are presented through Tables 3 to 6 and typical diagrams Fig.9 to Fig.11. The sampling rate of data acquisition was 0.01s, 0.1s, 1.0s and 3.6s. Accuracy is thus improved and the number of acquired data is reduced. In the Allan variance diagrams, the periods related to sampling rates are overlapped. The values presented in tables are best fitted values of different sampling rates.

Allan variance

The variance of two data points x_{j-1}, x_j relative to their mean is

¹⁾ Military Technical Institute (VTI), Ratka Resanovića 1, 11132 Belgrade, SERBIA

$$\left[x_{j-1} - \frac{x_{j-1} + x_j}{2} \right]^2 + \left[x_j - \frac{x_{j-1} + x_j}{2} \right]^2 = \frac{(x_j - x_{j-1})^2}{2} \quad (1)$$

Equation (1) motivates the definition of the Allan variance of data x_0, x_1, \dots, x_{N-1} taken at the time interval Δt to be the average of the variances of the data pairs x_{j-1}, x_j :

$$\sigma^2(\Delta t) = \frac{1}{2(N-1)} \sum_{j=1}^{N-1} (x_j - x_{j-1})^2 \quad (2)$$

Define a new sequence

$$y_j = \frac{x_{2j} + x_{2j+1}}{2}, \quad j = 0, 1, \dots, \left(\frac{N}{2}\right) - 1 \quad (3)$$

and compute the Allan variance $\sigma^2(2\Delta t)$ for this sequence. Iterating, the Allan variance $\sigma^2(n\Delta t)$ is calculated for longer and longer times $\tau = n\Delta t$, $n = 1, 2, 4, 8, \dots$. The square root of the Allan variance is then plotted versus the averaging time τ with log-log scales.

Power spectral density (PSD) of a stationary stochastic process

The PSD is the most commonly used representation of the spectral decomposition of a time series. It is a powerful tool for analyzing or characterizing data and stochastic modeling. The PSD, or spectrum analysis, is also better suited for analyzing periodic or aperiodic signals than other methods [3,1].

To summarize the basic relationship for stationary processes, the two-sided PSD, $S(\omega)$ and the covariance $K(\tau)$ is the Fourier transform pairs, related by:

$$S(\omega) = \int_{-\infty}^{+\infty} e^{-j\omega t} K(\tau) d\tau \quad (4)$$

$$K(\tau) = \frac{1}{2\pi} \int_{-\infty}^{+\infty} e^{j\omega\tau} S(\omega) d\omega \quad (5)$$

Unless specifically stated, the term PSD refers to the two-sided PSD. Graphical representations frequently use the one-sided PSD, whose amplitude is twice the two-sided PSD.

Covariance is defined by:

$$K[x(t_1, t_2)] = E[(x(t_1) - \mu(t_1))(x(t_2) - \mu(t_2))^T] \quad (6)$$

where μ is the mean value given by:

$$\mu(t) = E[x(t)] \quad (7)$$

For linear systems, the output PSD is the product of the input PSD and the magnitude squared of the system transfer function. If state space methods are used, the PSD matrices of the input and output are related to the system transfer function matrix $H(j\omega)$ by:

$$S_{yy}(\omega) = H(j\omega) S_{xx}(\omega) H^{*T}(j\omega) \quad (8)$$

where

$H^{*T}(j\omega)$ is the complex conjugate transpose of $H(j\omega)$. Thus, for the special case of white noise input, the output PSD directly gives the system transfer function.

The Fourier transform representation of the PSD is directly related to the bilateral Laplace transform derived from the transfer function of the corresponding stochastic model. The corresponding Allan variance of a stochastic process may be uniquely derived from its PSD; however, there is no general inversion formula.

The white noise covariance of process and measurement noise pertaining to the (continuous) Kalman Filter theory are identical to the corresponding two-sided PSD's white noise strengths expressed in units squared per Hertz $\left(\frac{(\text{unit})^2}{\text{Hz}}\right)$.

Power spectral density (PSD) and Allan variance relations

For the angular rates of the gyroscope output (Ω), the Allan variance is defined by

$$\sigma_\Omega^2(\tau) = \frac{1}{2(N-1)} \sum_{j=1}^{N-1} (\Omega_{k+1} - \Omega_k)^2 \quad (9)$$

and is related to the two-sided PSD, $S_\Omega(f)$ by:

$$\sigma_\Omega^2(\tau) = 4 \int_0^\infty S_\Omega(f) \frac{\sin^4(\pi f \tau)}{(\pi f \tau)^2} df \quad (10)$$

There is no inversion formula [4].

For accelerations (specific forces) of accelerometers (a), the Allan variance is defined by

$$\sigma_a^2(\tau) = \frac{1}{2(N-1)} \sum_{j=1}^{N-1} (a_{k+1} - a_k)^2 \quad (11)$$

and is related to the two-sided PSD, $S_a(f)$ by:

$$\sigma_a^2(\tau) = 4 \int_0^\infty S_a(f) \frac{\sin^4(\pi f \tau)}{(\pi f \tau)^2} df \quad (12)$$

Angle random walk

These noise terms are all characterized by a white noise spectrum of the gyro rate output (or accelerometer output). Fig.2 represents the PSD of an accelerometer approximated with the zero slope characteristic.

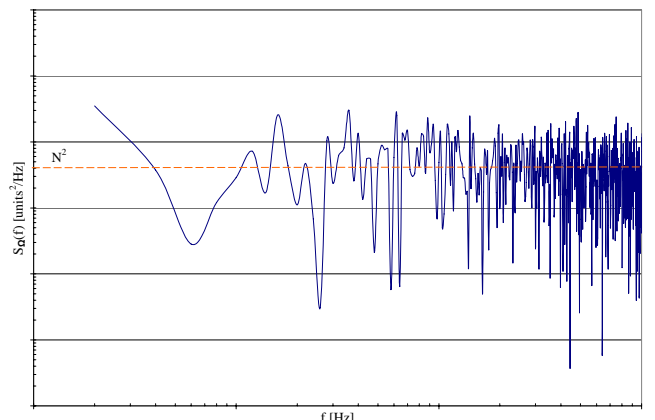


Figure 2. White noise spectrum of the gyro rate output

The rate noise PSD represented by Fig.2 is:

$$S_\Omega(f) = N^2 \quad (13)$$

where N is the angle random walk coefficient.

Substituting equation (13) in equation (10) yields:

$$\begin{aligned} \sigma_\Omega^2(\tau) &= 4 \int_0^\infty S_\Omega(f) \frac{\sin^4(\pi f \tau)}{(\pi f \tau)^2} df = \\ &= 4 \int_0^\infty N^2 \frac{\sin^4(\pi f \tau)}{(\pi f \tau)^2} df = \frac{N^2}{\tau} \\ \sigma^2(\tau) &= \frac{N^2}{\tau} \end{aligned} \quad (14)$$

The plot of equation (14) is presented in Fig.3. This plot indicates that a log-log slope of $\sigma(\tau)$ versus τ has a slope of $-1/2$.

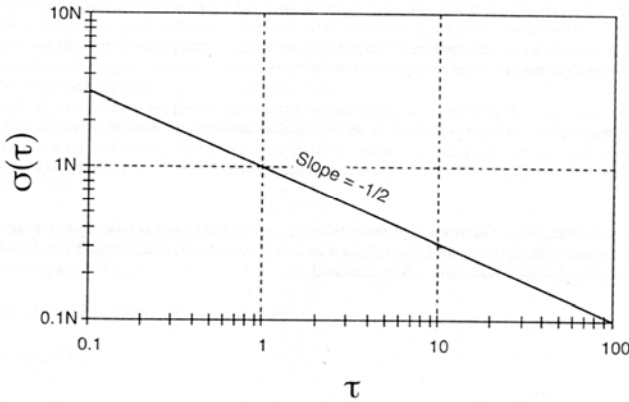


Figure 3. Plot for angle random walk

The solution of equation (14) for $\tau = 1$ s is:

$$\begin{aligned} N^2 &= \tau \sigma^2(\tau) = \sigma^2(1s) \\ N &= \sigma(1s) \end{aligned} \quad (15)$$

In equation (15) it can be remarked that numerical value for N is obtained by reading the slope line at $\tau = 1$ s.

The relation between the PSD (for gyro, $S_\Omega(f)$) and the angle random walk coefficient N is:

$$N(\text{°/h}) = \frac{1}{60} \sqrt{PSD \left[\frac{(\text{°/h})^2}{\text{Hz}} \right]} \quad (16)$$

Bias instability

The origin of this noise is electronic or other components susceptible to random flickering. Due to its low-frequency nature, it occurs as the bias fluctuation in the data. The rate PSD associated with this noise is [4]:

$$S_\Omega(f) = \begin{cases} \left(\frac{B^2}{2\pi}\right) \frac{1}{f} & f \leq f_0 \\ 0 & f > f_0 \end{cases} \quad (17)$$

where

B – bias instability

f_0 – cutoff frequency

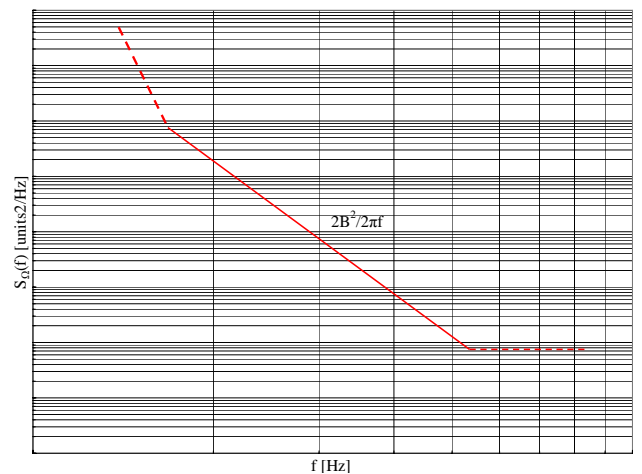


Figure 4. Representation of a hypothetical single-sided form

Substituting equation (17) in equation (10) yields:

$$\sigma^2(\tau) = \frac{2B^2}{\pi} \left[\ln 2 - \frac{\sin^3 x}{2x^2} (\sin x + 4x \cos x) + Ci(2x) - Ci(4x) \right] \quad (17)$$

where

x – is $\pi f_0 \tau$

Ci – is the cosine-integral function

Fig.5 represents a log-log plot of eq. 17.

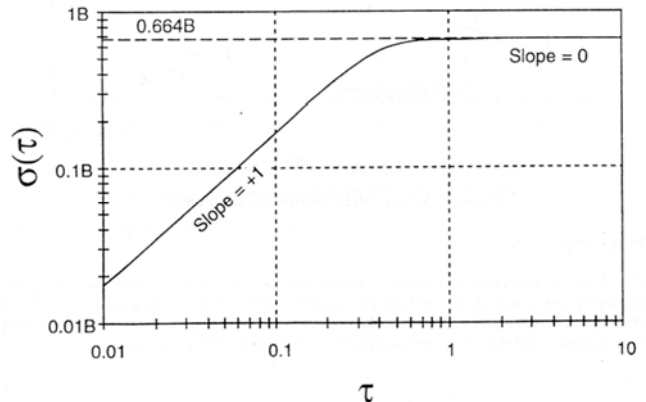


Figure 5. Plot of bias instability ($f_0 = 1$)

The plot in Fig.5 shows that the Allan variance for bias instability reaches a zero slope for τ much longer than the inverse of cutoff frequency. Thus, the flat region of the plot can be examined to estimate the limit of the bias instability as well as the cutoff frequency of the underlying flicker.

The slopes of typical PSD and Allan variance log-log diagrams are given in Table 1 [3].

Table 1. Slope of PSD and Allan variance coefficients

Signal	PSD	Square root Allan variance
Trend	-2	+1
Random walk	-2	+1/2
Flicker noise	-1	0
White noise	0	-1/2
Quantization noise	+2	+1

Sensor parameters identification

All measurements were done on the two-axis test table CARCO T-922, Fig.6, whose performances are: Minimum angular rate 0.0001 deg/s; maximum angular rate 999 deg/s and position accuracy 0.0001 degree. The ambient temperature was $22 \pm 1^\circ\text{C}$.

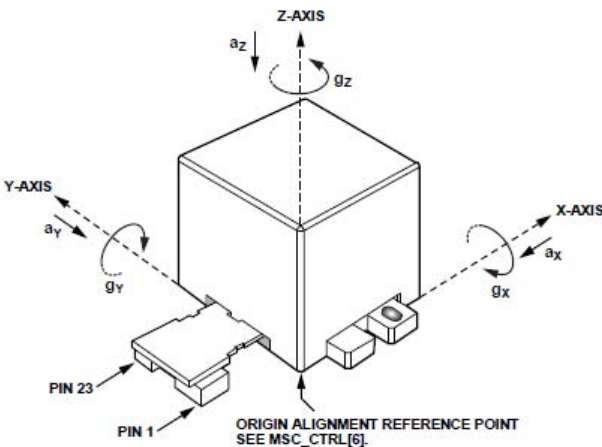
The Allan variance software for analyzing is made in accordance with (1), (2) and (3).



Figure 6. Two-axis test table



Figure 7. Sensor with the interface board



NOTES
1. ACCELERATION (a_x , a_y , a_z) AND ROTATIONAL (g_x , g_y , g_z) ARROWS
INDICATE THE DIRECTION OF MOTION THAT PRODUCES
A POSITIVE OUTPUT.

Figure 8. Sensor axis orientation

According to the scheme in Fig.1, a sensor is connected to the master processor through the interface board (ADIS16365/PCBZ), Fig.7. A completed unit is attached to the top of the inner test table axis. The axis z of the sensor, Fig.8, is positioned vertically upwards, the axis Y horizontally to the East and the axis X horizontally to the South.

In accordance with Fig.8, the accelerometer axes are denoted a_x , a_y and a_z , while the gyroscope axes are denoted ω_x , ω_y and ω_z .

Table 2 presents the data sheet specification of the analyzed parameters.

Table 2. ADIS 16365 parameters specification

Parameter	Test condition	Value	Unit
GYROSCOPES			
In-run Bias stability	1σ , SMPL_PRD=0x0001	0.007	$^\circ/\text{s}$
Angular random walk	1σ , SMPL_PRD=0x0001	2.0	$^\circ/\sqrt{\text{s}}$
ACCELEROMETERS			
In-run Bias stability	1σ	0.2	mg
Velocity random walk	1σ	0.2	$(\text{m}/\text{s})/\sqrt{\text{s}}$

The accelerometer velocity random walk and bias instability, and the gyroscope angle random walk and bias instability are identified by the Allan variance and the PSD. A number of 5010 data is acquired with the 0.01s sampling rate. A number of 1000 data is acquired with the 0.1 s, 1.0 s and 3.6 s sampling rates. The Allan variance of the acquired data for the y -axis is presented in diagrams in Fig.9 and Fig.10.

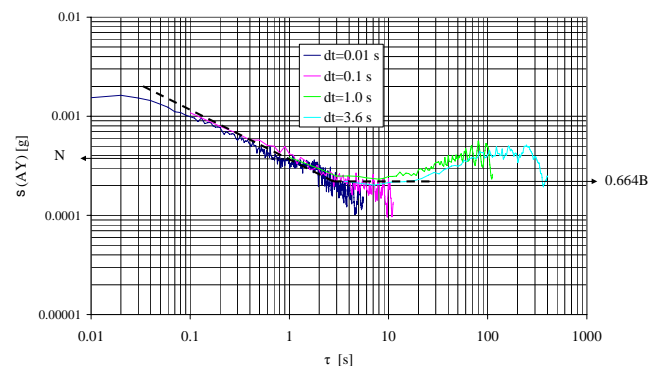


Figure 9. Square root Allan variance of the a_y accelerometer

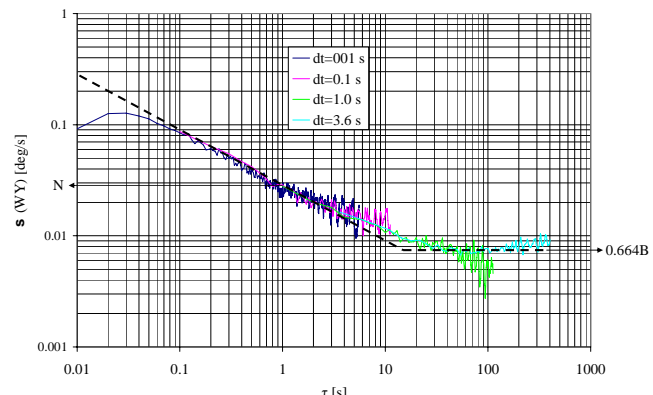


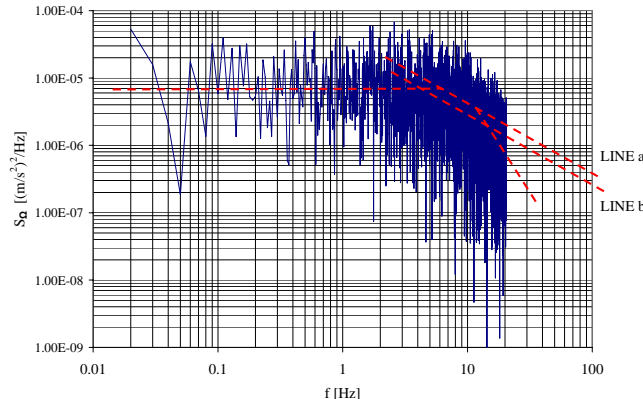
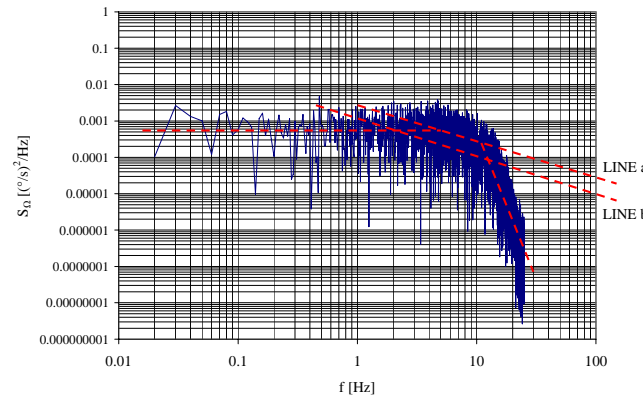
Figure 10. Square root Allan variance of the ω_y gyroscope

The sensor parameters determined from the Allan variance diagrams 9 and 10, are presented in Table 3.

Table 3. Sensors parameters determined from the Allan variance diagrams

Parameter	Determined from measurements	Data sheet value	Unit
ACCELEROMETER			
Velocity random walk coefficient $N(a_y)$	0.226	0.2	$\frac{m/s}{\sqrt{h}}$
Bias instability coefficient $B(a_y)$	0.304	0.2	mg
GYROSCOPE			
Angle random walk coefficient $N(\omega_y)$	1.68	2.0	$^{\circ}/\sqrt{h}$
Bias instability coefficient $B(\omega_y)$	0.0105	0.007	$^{\circ}/s$

The PSD of the acquired data for the y - axis is presented in diagrams in Fig.11 and Fig.12.

**Figure 11.** PSD of the a_y accelerometer**Figure 12.** PSD of the ω_y gyroscope

The sensor parameters determined from the PSD diagrams 11 and 12, are presented in Table 4.

Table 4. Sensors parameters determined from the PSD diagrams

Parameter	Determined from measurements	Data sheet value	Unit
ACCELEROMETER			
Velocity random walk coefficient $N(a_y)$	0.1587	0.2	$\frac{m/s}{\sqrt{h}}$
Bias instability coefficient $B(a_y)$	0.395 (line a) 0.1766 (line b)	0.2	mg
GYROSCOPE			
Angle random walk coefficient $N(\omega_y)$	1.34	2.0	$^{\circ}/\sqrt{h}$
Bias instability coefficient $B(\omega_y)$	0.0354 (line a) 0.00199 (line b)	0.007	$^{\circ}/s$

The bias instability coefficients are determined from the -1 slope linear characteristic in diagrams 8 and 9, using the equation:

$$\log\left(\frac{2B^2}{\omega}\right) = \log[S_a(f)] \quad (18)$$

$$\log\left(\frac{2B^2}{\omega}\right) = \log[S_\Omega(f)] \quad (19)$$

for the accelerometer, and for the gyro, respectively.

In diagrams Fig.11 and Fig.12, the two linear characteristics (line a and line b) are presented. The characteristics are chosen as margins of the diagram part where the observed trend is -1. This illustrates a possibility to choose many of the linear characteristics between these two lines, which gives a large difference for the calculated coefficients B. Usually choosing linear characteristic between these two lines.

The coefficients for the axes x and z of accelerometers and gyroscopes are determined similarly.

The results are presented in Tables 5 and 6 with the average values for the coefficient B.

Table 5. Sensors parameters determined from the Allan variance diagrams

Parameter	Determined value	Data sheet value	Unit
ACCELEROMETER			
Velocity random walk coefficient	$N(a_x) = 0.18944$	0.2	$\frac{m/s}{\sqrt{h}}$
	$N(a_y) = 0.22648$		
	$N(a_z) = 0.22356$		
Bias instability coefficient	$B(a_x) = 0.137$	0.2	mg
	$B(a_y) = 0.304$		
	$B(a_z) = 0.174$		
GYROSCOPE			
Angle random walk coefficient	$N(\omega_x) = 2.04$	2.0	$^{\circ}/\sqrt{h}$
	$N(\omega_y) = 1.68$		
	$N(\omega_z) = 1.86$		
Bias instability coefficient	$B(\omega_x) = 0.0135$	0.007	$^{\circ}/s$
	$B(\omega_y) = 0.0105$		
	$B(\omega_z) = 0.0120$		

Table 6. Sensors parameters determined from the PSD diagrams

Parameter	Determined value	Data sheet value	Unit
ACCELEROMETER			
Velocity random walk coefficient	$N(a_x) = 0.147$	0.2	$\frac{m/s}{\sqrt{h}}$
	$N(a_y) = 0.1587$		
	$N(a_z) = 0.1897$		
Bias instability coefficient	$B(a_x) = 0.322$	0.2	mg
	$B(a_y) = 0.2858$		
	$B(a_z) = 0.426$		
GYROSCOPE			
Angle random walk coefficient	$N(\omega_x) = 1.58$	2.0	$^{\circ}/\sqrt{h}$
	$N(\omega_y) = 1.34$		

	$N(\omega_z) = 1.47$		
Bias instability coefficient	$B(\omega_x) = 0.0418$	0.007	$^{\circ}/s$
	$B(\omega_y) = 0.018695$		
	$B(\omega_z) = 0.0132$		

Analysis of the experimental data

The analysis is done based on the data values acquired with a maximum sampling rate of 10 ms. With this sampling rate, using the PSD diagrams, we can conclude that accelerometer and gyro output noise is white noise in a range up to 10 Hz. The random walk and the bias instability are identified from the Allan variance and the PSD diagrams.

Both methods, the Allan variance and PSD, are suitable for the determination of the gyroscope angle random walk, the accelerometer velocity random walk and the bias instability coefficients for gyros and accelerometers.

The coefficients obtained by the Allan variance are slightly higher than those obtained by PSD. If we compare the values from the diagrams, we can conclude that it is much easier to read the values from the Allan variance plot than from the PSD plot. The reading of the angle random walk coefficients from the PSD plot is based on the mean value approximation of zero mean slopes. This is less accurate than those of the Allan variance plot which is in the cross-section of the diagram and ordinate for $\tau = 1s$.

The zero slope of the Allan variance plot is used for the determination of the coefficient B. From the PSD plot we use the -1 slope line. As mentioned earlier, there is a wide area on the plot where this line should be plotted. This is a source of unreliability of the coefficient B determined from this diagram.

Generally, we can conclude that it is more reliable to use the coefficients N and B for gyro and accelerometer noise obtained from the Allan variance plot than to use the coefficients obtained from the PSD plot. In spite of this, both methods must be used in the analysis in order to confirm that an appropriate coefficient is determined. Table 1 show that different coefficients have the same slope. Using the two methods, the Allan variance and PSD, it is possible to obtain a good estimation of coefficients.

The above analysis justifies the fact why the Allan variance plot is in most of manufacturers' data sheets.

Dve metode identifikacije parametara inercijalnih senzora

Inercijalni senzori, žiroskopi i akcelerometri imaju široku primenu. Inercijalni navigacioni sistemi (INS) se najčešće sastoje od inercijalnog mernog uređaja (IMU) sa tri medusobno upravna žiroskopa i akcelerometra koji predstavljaju tri ulazne ose sistema i navigacionog algoritma. Navigacioni algoritam koristi kao ulazne veličine signale žiroskopa i akcelerometara. Vema važno je poznavanje izvora grešaka u navigacionom algoritmu. Jedan od izvora je nestabilnost razdešenosti senzora. Nestabilnost razdešenosti je parametar koji definije klasu senzora. Klasa žiroskopa je definisana u $^{\circ}/h$ ili $^{\circ}/s$, a klasa akcelerometra je definisana u mg ili μg . Drugi parametri koji definisu slučajno odstupanje senzora su slučajno odstupanje ugla žiroskopa i slučajno odstupanje brzine akcelerometra. Iako proizvođači deklarišu navdene parametre u svojim katalozima, veoma je važno da se pre primene senzora potvrde svi parametri senzora. Prikazane su dve metode određivanja slučajnog odstupanja ugla, slučajnog odstupanja brzine i nestabilnosti razdešenosti žiroskopa i akcelerometra i prodiskutovana koja od metoda je tačnija. Ove dve metode su bazirane na Alanovoj disperziji i spektru gustine snage (SGS). Analiza je radena na šestokomponentnom mernom senzoru Analog Devices ADIS 16365.

Ključne reči: navigacioni sistem, inercioni sistem, inercijalna navigacija, inercijalni senzor, žiroskop, akcelerometar.

Conclusion

Experimental signal measurements of the six-degree sensor ADIS16365 were done. Based on the presented theoretical considerations, two methods of analysis were used to determine the angular random walk coefficient N and the bias instability coefficient B . It can be concluded that the application of the Allan variance method is easier and more precise than the power spectral density method.

References

- [1] *Six Degrees of Freedom Inertial Sensor ADIS16360/16365*, ANALOG DEVICES, <http://www.analog.com/en/sensors/inertial-sensors/adis16365/products/product.html>
- [2] IEEE Std 528-1994, IEEE Standard for Inertial Sensor Terminology, IEEE 1994.
- [3] IEEE Std 1293-1996, IEEE Standard Specification Format Guide and Test Procedure for Linear, Single -axis, Nongyroscopic Accelerometers, IEEE 1996.
- [4] IEEE 952-1997, IEEE Standard Specification Format Guide and Test Procedure for Single-Axis Interferometric Fiber Optic Gyros
- [5] Haiying Hou: *Modeling Inertial Sensors Errors Using Allan Variance*, A Thesis, Department of Geomatics Engineering, Calgary, Alberta, 2004
- [6] David W Allan and James A Barnes: *A Modified "Allan variance" with increased oscillator characterization ability*, Proc. 35 Ann. Freq. Control Symposium, USAERADCOM Ft. Monmouth, NJ 07703, May 1981.
- [7] Songlai Han, Jinling Wang, Nathan Knight: *Using Allan variance to determine the calibration model of inertial sensors for GPS/INS integration*, 6th International Symposium on Mobile Mapping Technology, Presidente Prudente, São Paulo, Brazil, July 21-24, 2009
- [8] Julius S. Bendat, Allan G. Piersol: *Random Data Analysis and Measurement Procedures*, Third edition, John Wiley & Sons, New York, 2000.
- [9] Zarchan,P.: *Fundamentals of Kalman filtering-A practical approach*, Second edition, American Institute of Aeronautics and Astronautics, Inc., Reston, Virginia, USA 2005.
- [10] Titterton,D.H., Weston,J.L.: *Strapdown Inertial Navigation Technology*, American Institute of Aeronautics and Astronautics, Inc, 2009.

Received: 13.11.2010.

Два метода идентификации параметров инерционных датчиков

У инерционных датчиков, гироскопов и акселерометров очень широкое применение. Инерционные навигационные системы (ИНС) больше и чаще всего состоят из инерционного измерительного прибора (ИИП) со тремя взаимно перпендикулярными гироскопами и акселерометрами, которые представляют три входные оси системы и навигационного алгорифма. В роли входных величин навигационный алгорифм пользуется сигналами гироскопа и акселерометров. Очень важной является познавательность источника ошибок в навигационном алгорифме. Одним из источников является неустойчивость погрешности датчика. Неустойчивость погрешности является параметром определяющим класс датчиков. Класс гироскопов определён в $^{\circ}/\text{h}$ или $^{\circ}/\text{s}$, а класс акселерометров определён mg или μg ($\text{g} \approx 9.81 \text{ m/s}^2$). Остальные параметры, определяющие случайное отклонение датчиков, это случайное отклонение угла гироскопа и случайное отклонение скорости акселерометра. В зависимости от применения и обязательной точности датчика, конструкторы выбирают определённый датчик. Все изготовители объявляют приведённые параметры в своих ведомостях. Несмотря на объявленные значения параметров, очень важно чтобы перед применением датчика измерить все параметры с целью устранения некоторых из них и с целью проверки качества датчика. Здесь показаны два метода определения случайного отклонения угла, случайного отклонения скорости и неустойчивости погрешности гироскопа и акселерометра и обсуждено какой из методов является более пунктуальным. Эти два метода обоснованы на изменении Аллана и на спектральной плотности мощности (СПМ). Анализ проведён на шестиступенчатом измерительном датчике Analog Devices ADIS 16365.

Ключевые слова: навигационная система, инерционная система, инерционная навигация, инерционный датчик, гироскоп, у акселерометр.

Deux méthodes pour l'identification des paramètres chez les capteurs inertIELS

Les capteurs inertIELS, gyroscopes et accéléromètres, ont une grande application. Les systèmes inertIELS de navigation (SIN) se composent le plus souvent d'un appareil inertIEL de mesure avec trois gyroscopes mutuellement perpendiculaires et un accéléromètre qui représentent trois axes d'entrée du système et de l'algorithme de navigation. Il est très important de connaître les sources des erreurs chez l'algorithme de navigation. L'instabilité du déréglage du capteur est l'une de ces sources. L'instabilité du déréglage est le paramètre qui définit la classe du capteur. La classe du gyroscope est définie par le degré/h ou le degré/s tandis que la classe de l'accéléromètre est définie en mg ou μg . Les autres paramètres qui définissent la marche aléatoire du capteur sont : l'écart aléatoire de l'angle du gyroscope et la marche aléatoire de la vitesse de l'accéléromètre. Bien que tous les producteurs déclarent les paramètres cités dans leurs catalogues il est très important de prouver tous les paramètres avant l'emploi du capteur. On a présenté deux méthodes pour la détermination de l'écart aléatoire de l'angle, l'écart aléatoire de la vitesse et l'instabilité du déréglage de gyroscope et l'accéléromètre et on a discuté quelle méthode est plus précise. Ces deux méthodes sont basées sur la dispersion d'Alan et le spectre de la densité de force. L'analyse a été faite sur le capteur de mesure à six composantes Analog Devices ADIS 16365.

Mots clés: système de navigation, système inertIEL, navigation inertIELle, capteur inertIEL, gyroscope, accéléromètre.